American Journal of Nanosciences
2019; 5(1): 9-17
http://www.sciencepublishinggroup.com/j/ajn
doi: 10.11648/j.ajn.20190501.12
ISSN: 2575-484X (Print); ISSN: 2575-4858 (Online)

Characterization of Multinanoporous Pt-TiO_2 Thin Films Fabricated by a Three-Step Electrochemical Technique

Ekoko Bakambo Gracien[1, *], Muswema Lunguya Jérémie[1], Mbongo Kimpanza Antoine[1], Nzazi Kambamba Nicole[2], Nduku Mafwa Fabrice[3], Musengele Bilasi Denis[3], Kidingi Kambasi Pierre[4], Ndonganzadi Tresor[3], Mukiatom Perbom[5]

[1]Department of Chemistry, University of Kinshasa, Kinshasa, Democratic Republic of the Congo

[2]Department of Biological Chemistry, High Educational Institute of Kitoy, Masimanimba, Democratic Republic of the Congo

[3]Department of Physical Chemistry, High Educational Institute of Kikwit, Kikwit, Democratic Republic of the Congo

[4]Department of Biological Chemistry, High Educational Institute of Dula, Bulungu, Democratic Republic of the Congo

[5]Department of Construction, Institute of Construction and Public Works of Kikwit, Kikwit, Democratic Republic of the Congo

Email address:
profekokob@yahoo.fr (E. B. Gracien)

[*]Corresponding author

To cite this article:
Ekoko Bakambo Gracien, Muswema Lunguya Jérémie, Mbongo Kimpanza Antoine, Nzazi Kambamba Nicole, Nduku Mafwa Fabrice, Musengele Bilasi Denis, Kidingi Kambasi Pierre, Ndonganzadi Tresor, Mukiatom Perbom. Characterization of Multinanoporous Pt-TiO_2 Thin Films Fabricated by a Three-Step Electrochemical Technique. *American Journal of Nanosciences.* Vol. 5, No. 1, 2019, pp. 9-17.
doi: 10.11648/j.ajn.20190501.12

Received: July 3, 2019; **Accepted**: July 24, 2019; **Published**: August 13, 2019

Abstract: In the present investigation, a three-step electrochemical as a novel method has been applied to fabricate multinanoporous thin film electrodes of pure TiO_2 and the doped Pt-TiO_2 (of approximately 15 nm) from the titanium sheet using sulfuric acid as electrolyte and chloroplatinic acid as platinum dopant precursor. Characterization techniques so far discussed in this work revealed that the fabricated products corresponded to pure TiO_2 and to the doped Pt-TiO_2 respectively. The prepared Pt-TiO_2 thin film electrodes have photoresponse to visible light, which indicates a new possibility for improving intrinsic TiO_2 photoresponse.

Keywords: Pt-TiO_2 Films, Anodic Oxidation, Visible Photo Response, Doping

1. Introduction

Titanium dioxide has three polymorphic crystal structures (brookite, anatase and rutile) and its photocatalytic activity is crystal structure dependent. The anatase with an energy band of about 3.2 eV has various scopes of application.

The TiO_2 in anatase structure has been extensively investigated in the field of photocatalysis. Unfortunately its use in wastewater treatment is limited due to the low energy conversion efficiency (< 5%). When TiO_2 is illuminated by ultraviolet light, the majority of the UV induced generated charge carriers (electrons: e^- and holes: h^+) in the lattice undergo rapid recombination before they reach the surface of the semiconductor and then interact with the adsorbed molecules. These photogenerated charge carriers recombination becomes the main barrier in the development of the photocatalytic technology [1].

The photocatalytic activity of this semiconductor material can be remarkably ameliorated by doping with noble metals (Pt), which plays the role of pulling electrons into its lattice and acts as the photogenerated electron acceptor. This electron's scavenging efficaciously delays the charge carrier's recombination by improving the quantum yield and the photocatalytic efficiency. On the semiconductor surface the holes typically generate hydroxyl radical species ($^{\bullet}OH$) that are among the strongest oxidizers known (the standard electrode potential: 2.8V) [2-6].

Researchers have designed systems in which the fine (doped or undoped) TiO_2 photocatalyst powder was dispersed in liquid suspension. However, this technology could not work continuously because, after the degradation process under UV light irradiation, the photocatalyst powder

remains suspended in water. The use of filters or sedimentation methods to remove TiO_2 powders has been proved to be inefficient and cost-effective.

For this reason, a TiO_2 fixed system is needed in order to avoid such bath operation and continuous wastewater treatments become more practical. Several investigators have dealt with the development of procedures for catalyst immobilization on solid material surfaces.

The sol-gel, the pulsed laser deposition and other methods have been generously employed to incorporate transition metals in titanium dioxide. However, in most of these methods, the doped titanium dioxide are fabricated from powder and paste on any conductive substrates and, then finally dry or heat with the purpose to fabricate the desired doped- TiO_2 electrodes. Therefore, TiO_2 has been affixed to a variety of surfaces: glass; silicon; clays; organic polymers; thin films; concrete; alumina and carbon [7-11]. The use of these fabricated thin films doped- TiO_2 as electrodes in water cleaning process was shown to be advantageous but their stability is not sufficient for economic use. They have shown a remarkably decay of their photocatalytic efficiency after several re-use. Then, a method which can be designed to prepare of the highly photoactive and mechanically stable multinanoporous TiO_2 thin films is a requirement for the development of practical photocatalytic reactors for the treatment and water purification.

Metal deposition by electrochemical technique is generously used to prepare nanostructured materials on solid material surfaces. To produce the desired thin film thickness, one has to control the particle size or the shape, and the morphology of the deposited metal by adjusting and optimizing electrochemical conditions such as the deposition time, the electrode applied potential, and electrolyte nature. Contrary to electrochemical metal deposition on metal or semiconductor supports, deposition on oxide surfaces has seldom been realized and has been limited only to oxide thin films produced on conductive substrates probably due to insufficient conductivity of oxide itself [12].

Nevertheless, the deposition of metal on an oxide surface is mandatory for applications such as oxide-supported metal catalysts, where the catalytic properties are mostly dependent both on the metal particle size or shape and on the strength of the metal support interaction.

Consequently, electrochemical metal deposition on an oxide surface could certainly be a promising technique to obtain well-controlled nanoparticles on oxide surfaces.

Lately, various methods have been reported for the synthesis of Pt/ TiO_2 electrodes [1, 2, 13-17].

In recent years, the electrochemical anodic oxidation method was carefully used in our laboratory to optimize the experimental parameters in the synthesis of the photocatalytic thin films made of intrinsic TiO_2 on one hand [18-19]. And on the other hand, unfilled d-levels transition metals (Fe, Mn, Cr, Co and Ni) were incorporated into TiO_2 with the aim of improving the photocatalytic properties of the fabricated doped-TiO_2 multinanoporous thin films [20]. The experimental results revealed that the photocatalytic properties of transition metal doped-TiO_2 greatly depend on the nature of the metal used as dopant. The influence of these experimental parameters on the structure, morphology and photocatalytic activity of the TiO_2 films was systematically evaluated. The internal relationship between the structure and property of the TiO_2 film was analyzed and the obtained results were reported [21-23].

In the present work, a three-step electrochemical technique for the preparation of electrochemical-deposited platinum metal on anatase TiO_2 electrodes is developed. Its originality relies on the fact that the conductive titanium sheet is used as the starting material to produce firstly titanium dioxide films on titanium sheet by anodic oxidation. And secondly, the metal doping is made directly from the produced oxide and finally, the whole system is immobilized on the titanium substrate. This method is more preferable than slurry or suspension systems, due to easy and convenient catalyst handling. The need of post-treating (centrifugation or filtration) to separate the catalyst from the reaction mixture is eliminated. The photocatalytic activity of the prepared electrodes on the oxidation of an aqueous solution of methanol was investigated.

2. Experimental Method

2.1. Samples Preparation

All the reagents used in the present investigation were analytical grade with minimum assay 95% and were purchased from Shanghai Chemical Reagent Co., Shanghai, China. They were used as received, without further purification. The following chemical reagents were used for the fabrication of pure and doped titania electrodes: Titanium plates of 0.5 mm thick (containing $N \leq 0.012\%$, $C \leq 0.02\%$, $Si < 0.04\%$ and $Fe \leq 0.06\%$); hydrofluoric acid (HF 4% concentration); sulfuric acid (H_2SO_4, 98%); boric acid (H_3BO_3, > 99%); sodium sulfate (Na_2SO_4, > 99%); chloroplatinic acid (H_2PtCl_6, > 99%); isopropyl alcohol or 2-propanol (CH_3-CHOH-CH_3, 98%); sodium hydroxide (NaOH, > 99%); methanol (CH_3OH, 98%); ethanol (absolute alcohol, CH_3CH_2OH, 98%); acetone or propanone (CH_3-CO-CH_3, 98%); sodium chloride (NaCl, > 99%); disodium ethylene diamine tetraacetate (molecular formula: $C_{10}H_{14}N_2O_8Na_2$. H_2O, > 99%) or Na_2 (EDTA) or $Na_2H_2Y^{4-}$ with [Y = $[_2(OOC)\ NCH_2CH_2N\ (COO)_2]^{4-}$]) and the azo dye, acid orange 7 (7-hydroxy -8- (phenylazo)-1,3-naphtalene disulfonic acid disodium salt, molecular formula: $C_{16}H_{10}N_2O_7S_2Na_2$, 87-95%) or Na_2 (EDTA). The latter was used to enhance the solubility of free Pt^{4+} ions in aqueous solution.

In the present work, in order to check the possibility of enhancing the photocatalytic activity of TiO_2, noble platinum metal was incorporated on TiO_2 by using a three-step electrochemical technique. This technique for producing Pt-TiO_2 thin films consists of:

1) Anodization at ambient temperature of titanium sheet in oxalic acid 0.8 mole/L solution at very high current density (90-100 mA/cm^2) and low voltage (60 V) for 3 minutes in order to produce a conductive porous coating layer of titanium dioxide over the entire surface of titanium film. The produced film accessible for

subsequent incorporation of transition metals by electrodeposition method.

2) Incorporation of noble platinum metal in to the previously prepared conductive porous titanium dioxide by electrodeposition under high current density of about 75-90 mA/cm^2. The high current density was applied for enhancing adhesion of platinum into the coating layer. Boric acid (10 g/L) was added in the bath to increase the conductivity (lessen high current density burning) and thus preventing the precipitation of the metal hydroxides. Chloroplatinic acid (350mg/L) was used as precursor to provide a metal doping agent in ionic form. The Na_2 (EDTA) was added in the metal ion solution to increase the solubility of metal through anionic complex formation. The solution pH was kept about 2.0 since the TiO_2 in acidic medium is positively charged. Therefore, anionic complexes formed from EDTA and transition Pt^{4+} ions were electrostatically bound to the TiO_2 surface. Disposable electrons reduced the Pt^{4+} ions to zero valence Pt which plates out on the pre-anodized TiO_2 surface with good adherence and subsequently these electrodes are used to produce stable multinanoporous thin-films of titanium dioxide.

The electrodeposition time of platinum metal on TiO_2 could varied from 1 to 5 minutes (refer to Table 1). In this manner the adherence of platinum on the surface of TiO_2 is controlled and subsequently these electrodes are used to produce stable platinum doped thin-films of multinanoporous TiO_2.

3) After doping the pre-anodized titanium dioxide with platinum metal, the doped product was then re-anodized at room temperature for 5 minutes by direct current in sulfuric acid 0.1 mol/l as electrolyte at high voltage (130 V with a current density of about 15-20mA/cm^2). The cathode was made of graphite. Multinanoporous films constituted of Pt- TiO_2 were produced. The fabricated thin films were immediately rinsed with distilled water to remove the byproducts and then, they were dried in air and characterized by analytical equipments.

Table 1. *The metal concentration in Pt-TiO_2 electrodes produced under different electrodeposition time by using a three-step electrochemical technique.*

Electrode	Electro deposition time (min)	Metal concentration in TiO_2 (at.%)
Pt-TiO_2	0.25	0.15 ± 0.03
	0.50	0.32 ± 0.02
	1.00	0.51 ± 0.02
	1.50	0.58 ± 0.01
	2.00	0.73 ± 0.02
	3.00	1.05 ± 0.01
	3.50	1.23 ± 0.01
	4.00	1.56 ± 0.03
	5.00	2.23 ± 0.03

*The concentrations are expressed as atomic percent (at.%) and are the average of three independently measurements made at three different points of the electrode under study (± standard deviation).

2.2. Characterization Techniques

All reagents and solvents for the preparationn and analysis were pure and were used as received without further purifications. The structure and the phase identification of the prepared materials was carried out on X-ray powder diffraction (XRD) patterns, using a D/MAX-2550 Xray diffractometer with Cu-Kα radiation (λ=1.54056 Å) with a nickel filter (Rigaku Co., Japan). The crystalline sizes were calculated by using the Debye- Scherrer formula. The chemical bondings in the prepared TiO_2 thin films were recorded by Fourier transform infrared spectra (SHIMADZU Spectrophotometer) using KBr pellet technique in the range from 4000 cm^{-1} to 400 cm^{-1}. The surface morphology, size of particles and elemental compositions of TiO_2 electrodes were carried out by field emission scanning electron microscopy (FE-SEM; JEOL JSM-6700F) well equipped with an energy dispersive X-ray (EDAX) spectrophotometer and operated at 20kV. The chemical bonding on the thin films surface was studied using X-ray photoelectron spectroscopy (XPS), which was performed with a Thermo VG Scientific ESCALAB 250 spectrometer with a monochromatized Al-Kα X-ray source (1486.6 eV energy). The morphology of the synthesized TiO_2 electrodes was determined by transmission electron microscopy (TEM; Hitachi H-800), and selected area electron diffraction (SAED). The TEM micrographs were taken with an accelerating voltage of 200 kV with samples deposited on a carbon coated copper grid. The wavelength of electron in this condition was approximately about 2.5× 10^{-12} m and the camera length was fixed at 170 cm for the selected area electron diffraction. The optical properties of the prepared electrodes were analyzed by UV–Vis absorption spectra in the wavelength range of 300–800 nm. The diffuse reflectance spectra of the undoped TiO_2 and Pt–TiO_2 film electrodes were recorded by a Shimaszu spectrophotometer (model: UV-PC3101PC) with an integrating sphere (Specular Reflectance ATT. 5DEG) in which the baseline correction was done using a calibrated sample of barium sulfate. And finally, compositional and structural investigations throughout the thin film electrodes after several uses were performed through Raman measurements, which were perform at room temperature with a Spex1403 laser Raman scattering spectrometer. The laser power was kept low in order to avoid undesired heating effects on the samples.

3. Results

3.1. Characterization of Intrinsic TiO_2 and Pt Doped TiO_2 Multinanoporous

The compositions of the as-prepared intrinsic TiO_2 and Pt doped TiO_2 multinanoporous samples were revealed by XRD.

Figure 1 shows XRD patterns of pure TiO_2 and Pt-TiO_2 thin films prepared by a Three-Step Electrochemical Technique (platinum concentration: 1.05%).

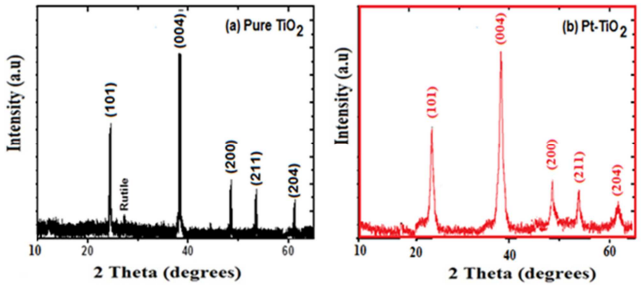

Figure 1. *X-ray patterns of (a): pure TiO_2 films (synthesis conditions: Anodization voltage: 130V, electrolyte: H_2SO_4 1.0 mol/L; anodization time: 5min; temperature: 25°C; current density: 15-20 mA/cm²) and (b): Pt-doped TiO_2 electrode (Pt concentration: 1.05%). The various Bragg peaks are followed by the corresponding Miller indices. Results were obtained using Cu K_α radiation (λ= 1.54178Å).*

The influence of platinum concentration doped in the semiconductor material is shown in Figure 2.

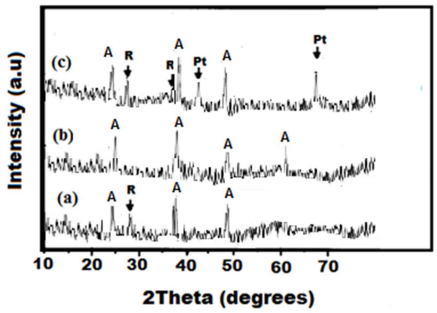

Figure 2. *X-ray patterns of (a): pure TiO_2, (b): Pt- TiO_2 electrode (Pt: 1.05 at.%), and (c): Pt- TiO_2 electrode (Pt 2.23 at.%). The various Bragg peaks are followed by A: anatase, R: rutile, Pt: PtO_2. Results were obtained using Cu K_α radiation (λ= 1.54178Å).*

3.2. Electrodes Morphology

Figure 3 shows the SEMs micrographs which describe the surface morphologies of the prepared samples following the three electrochemical steps which lead to the synthesis of multinanoporous Pt-TiO_2 thin film electrodes.

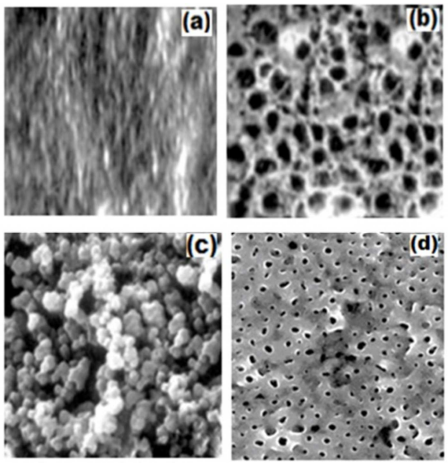

Figure 3. *SEM micrographs (a): Ti plate; (b): Ti film after anodization in oxalic acid 0.8 mole/L; (c): The platinum deposits on the pre-anodized porous film of TiO_2 and (d): Pt-TiO_2 electrode prepared by re-anodization technique (Pt concentration: 1.05%).*

3.3. Electron Diffraction Analysis

Electron diffraction was performed to further confirm the structure of the Pt-TiO_2 thin films electrodes. Samples for analysis were prepared by dissolving Pt-TiO_2 electrodes in an aqueous solution of HF (2%) for 2 minutes; the coat was separated from the Ti sheet and dried in air for several hours. Finally, the coat-dried powder was dispersed in absolute alcohol using an ultrasonic excitation, and was transferred onto the copper grid with a carbon support film for electron diffraction investigations. Figure 4 shows the electron diffraction micrograph of the prepared material. The lattices spacing (d) corresponding to the radius (r) of each ring of diffraction were calculated using the formula $r\,d = L\,\lambda$. The wavelength (λ) of electron in this condition was approximately about 2.5×10^{-12} m and the camera length (L) was fixed at 170 cm for the selected area electron diffraction. The L λ value was calibrated using the known structure of a polycrystalline gold thin film that was deposited onto an amorphous carbon substrate.

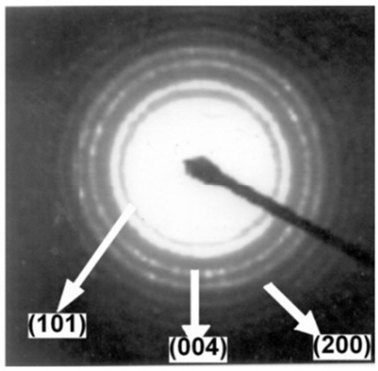

Figure 4. *Electron diffraction micrograph of the Pt-TiO_2 thin films prepared by re-anodisation technique (platinum concentration: 1.05%).*

Figure 4 shows the electron diffraction micrograph of the Pt-TiO_2 electrode sample.

3.4. Energy Dispersive Studies (EDS)

EDS analysis of the prepared Pt-TiO_2 thin film electrodes was carried out by using internal standard at energy from 0 to 10 keV. Energy dispersive X-ray spectroscopy (EDS) of Pt–TiO_2 is shown in Figure 5.

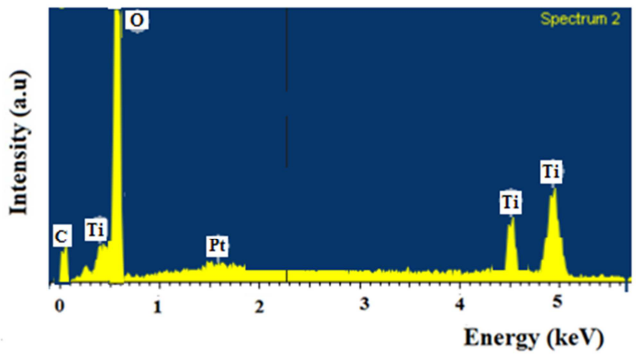

Figure 5. *Energy dispersive X-ray spectrum of of the prepared Pt- TiO_2 (Pt concentration: 1.05%).*

3.5. FT- IR Spectroscopy Analysis

FT- IR spectroscopy (investigated region: 4000-400 cm^{-1}) was carried out in order to ascertain the purity and nature of metal oxide thin films. The FT-IR spectrum of as-synthesized doped Pt-TiO_2 is indicated in Figure 6.

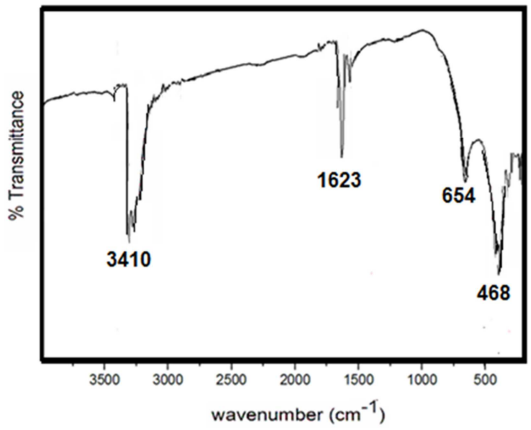

Figure 6. *The FT-IR spectrum of as-synthesized Pt-TiO_2 electrode (Pt concentration: 1.05%).*

3.6. Chemical Valence States by X-Ray Photoelectron Spectroscopy

To more endorse the chemical nature of the prepared Pt-TiO_2 multinanoporous, X-ray Photoelectron Spectroscopy was carried out and the result is shown in Figure 7.

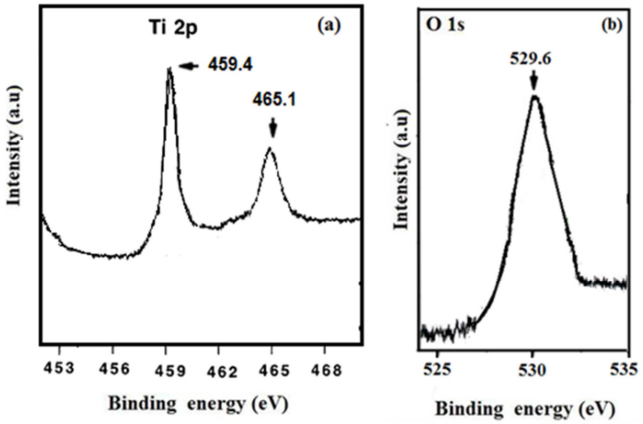

Figure 7. *XPS spectra of (a) Ti 2p and (b) O1s core levels of Pt-TiO_2 thin film electrode (Pt concentration: 1.05%).*

3.7. Effect of the Platinum Dopant Concentration on the Photocatalytic Activity of TiO_2 Electrodes

It was reported previously that, the application of an external potential bias helps to drive away the photogenerated electrons and consequently reducing the electron-hole recombination and the best value was about 3.5 V [22].

The CH_3OH was used a model pollutant in aqueous solutions under UV light at 365 nm using the prepared thin film electrodes. To test the effect of platinum metal doping TiO_2 electrode on the oxidation of of CH_3OH 0.2 mol/L + Na_2SO_4 0.3 mol/L (used as supported electrolyte), films of Pt -TiO_2 (with a total electrode surface area of about 95 cm^2) were used as a photoanodes. These electrodes were immersed in a photoreactor containing the CH_3OH, and a circular electrode made of graphite was used as the counter electrode. The applied potential bias could vary from 0.5 V to 5.0. Figure 8 shows the current-potential curves of TiO_2 and of Pt -TiO_2 electrodes (Pt concentration varying from 0.21 at% to 2.23 at%) under the illumination of UV light at 365 nm of CH_3OH solution.

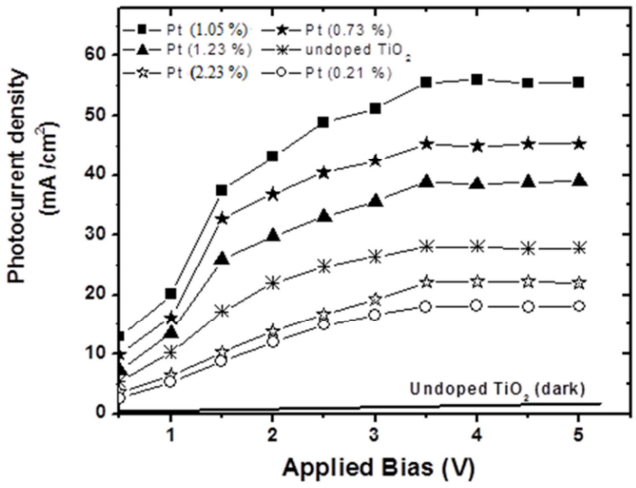

Figure 8. *The current-potential of intrinsic TiO_2 and Pt-TiO_2 electrodes under the illumination of UV light at 365 nm of CH_3OH solution.*

The photocurrent densities recorded as a function of Pt metal concentration in TiO_2 thin films is shown in Figure 9.

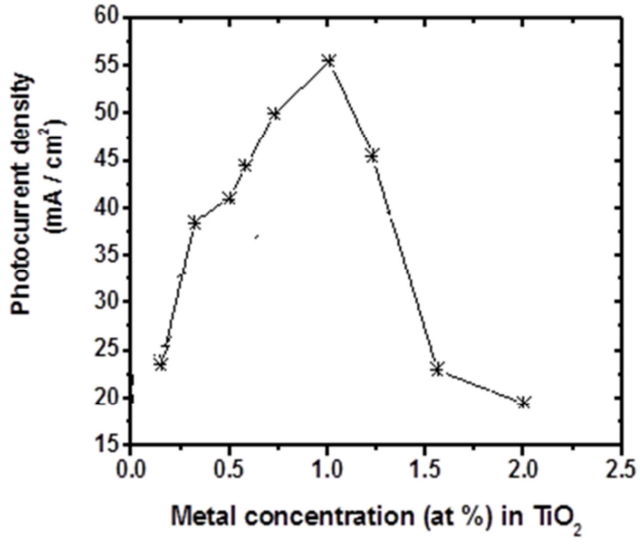

Figure 9. *The photocurrent density as a function of platinum concentration doped TiO_2 electrodes measured under the illumination UV at 365 nm (the area of electrode film is 95 cm^2 illuminated by the side, applied bias: 3.5V).*

3.8. Optical Properties of Transition Pt- TiO_2 Electrodes

The optical properties of the undoped TiO_2 and the Pt- TiO_2 electrodes were analyzed by UV–Vis absorption spectra in the wavelength range of 300–750 nm as shown in Figure 10.

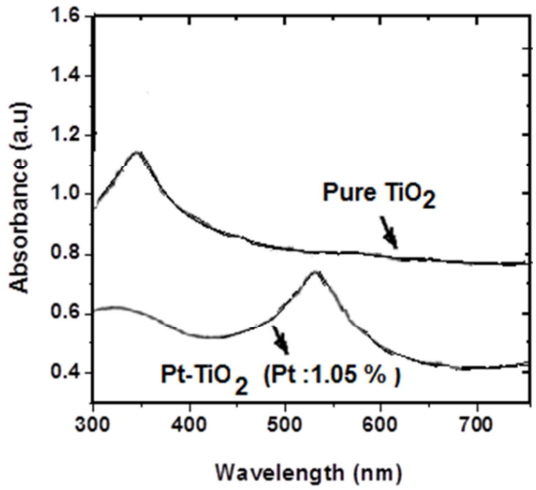

Figure 10. *The diffuse reflection spectra of the pure TiO_2 and Pt–TiO_2 thin film electrodes.*

3.9. Electrodes Composition After Methanol Oxidation

Figure 11 shows the Raman scattering spectrum of Pt-TiO_2 electrode after several uses in the methanol photodegradation process.

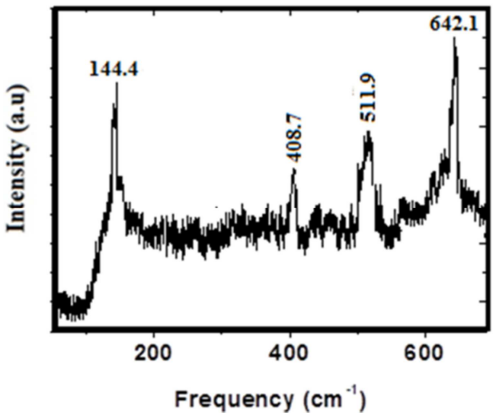

Figure 11. *Raman spectrum of Pt-TiO_2 electrode (Pt concentration: 1.05%) after methanol photo oxidation.*

4. Discussion

From Figure 1, one can notice that all diffraction peaks at 2θ (degrees) at about 25.3 (1 0 1), 38.1 (0 0 4), 48.3 (2 0 0), 55.1 (2 1 1) and 62.9 (2 0 4), displayed on the XRD patterns of the produced thin films, show that the produced electrodes (intrinsic TiO_2 and the Pt-TiO_2) exist mostly in anatase phase (JCPDF number: 21-1272).

On the whole, these diffraction peaks are sharp, narrow and symmetrical with a low and stable baseline, suggesting that the samples are single phased in the anatase structure.

In comparison with XRD pattern of pure TiO_2, Pt (platinum concentration: 1.05%) incorporated on TiO_2 surface nearly has not influence on crystalline structure and particle size. Platinum phase has not been detected in the XRD pattern of Pt-TiO_2 thin films, due to the platinum concentration on TiO_2 surface, which is not enough to form clearly a second crystalline phase. This suggests that there is no metal segregation in amounts large enough to be detected by XRD. This means that the Pt nanoparticles are isolated in Pt-TiO_2 nanoporous films, indicating that each Schottky barrier between Pt nanoparticles and TiO_2 is localized into the TiO_2 matrix.

The average diameter (D) of the synthesized Pt-TiO_2 multinanoporous has been calculated using Debye Scherrer's equation:

$$D = \frac{0.9\lambda}{\beta \cos\theta} \quad (1)$$

D was found to be about 15.2 nm (while the one calculated for the pure TiO_2 was about 14.6 nm). In Scherrer's equation 0.9 is a constant, λ is the wavelength of the X-rays (λ= 1.54178Å) and β is the full width at half maximum (FWHM) of the diffraction peaks and θ is the diffraction angle.

From Figure 2, it can be seen that, an increase of Pt concentration up to 2.23 at.% leads to the formation a new phase constituted of PtO_2 (refer to peaks located at 2θ (degrees) = 39.8 and 46.6) while at Pt concentration of about 1.05 at.%, only one phase made of anatase TiO_2 could be observed. We suggest that, the decrease of the photocatalytic activity of TiO_2 when doped with higher metal content could be due to formation of the second phase, which is inhibiting the photocatalytic activity of anatase TiO_2.

From Figure 3, It can be clearly seen that after anodization of titanium sheet (Ti) with oxalic acid 0.8 mol/l, a thin and porous film was obtained in order to support the platinum metal deposition process.

At current density of 75 mA/cm^2 (pH 2.0, 40 ˚C), platinum metal was deposited on the pre-anodized TiO_2 multiporous film. The platinum deposits were spherical crystals refering to Figure 3 (c). From Figure 3 (d), it is clearly observed that the fabricated electrode showed a multi-porous morphology. The pores can act as an absorption center for the photocatalytic reaction and are beneficial to the improvement of the photocatalytic activity.

The lattices d-spacing of the planes causing diffraction from figure 4 were calculated and are listed in Table 2. The calculated d-spacings from peaks (101), (004) and (200) related to TiO_2 anatase phase correspond well to the d-spacings values obtained from the XRD patterns. This indicates furthermore that the sample the prepared sample is constituted of TiO_2 in anatase structure.

Table 2. *The calculated d-spacing from peaks (101), (004) and (200) by electron diffraction.*

2θ	Diffraction planes	d-space from XRD (Å)	Radius of the diffraction ring (cm)	d-space calculated (Å)
25.3^0	(101)	3.55	1.2	3.54
38.1^0	(004)	2.36	1.8	2.36
48.3^0	(200)	1.89	2.3	1.85

The figure 5 confirms the presence of Ti, O and Pt. The experimental atomic percentages of Ti, O and Pt are respectively found to be 31.26%, 65.71% and 1.05%. The ratio of Ti and O is near to the theoretical ratio (1: 2) of TiO_2. The EDX spectrum supports others characterization techniques in confirming the presence of Pt-TiO_2 in the fabricated sample.

The FT- IR peaks (in Figure 6) at 468 cm^{-1} and 650 cm^{-1} are for O-Ti-O bonding. The broad absorption bands between 400 cm^{-1} and 800 cm^{-1} are mainly attributed to the anatase structure (Ti-O and O-Ti-O flexion vibration) [24, 25]. Upon addition of dopant, a small shift was detected for the stretching vibration of Ti–O [26]. The two bands appeared at about 3410 and 1623 cm^{-1} have been assigned respectively to the stretching and binding vibrations of absorbed water molecules on Pt-TiO_2 mutinanoporous particles [24, 25].

By analysing the pattern of the Ti 2p in pure TiO_2 showed peaks located at 454.1 and 464.7 eV corresponding to the Ti $2p_{3/2}$ and Ti $2p_{1/2}$. The main contribution to the formation of XPS Ti 2p-spectra comes from tetravalent state titanium (Ti^{4+}) due to formation of Ti-O bonds similar to those in stoichiometric TiO_2. The pattern of the Ti 2p in Pt-TiO_2 exhibited for the titanium atom, two distinct peaks at 459.4 eV for the Ti $2p_{1/2}$ and at 465.1 eV for the Ti 2p3/2, both in good agreement with the database [27].

In comparison with the pure TiO_2 electrode, the Ti 2p peak at 459.4 eV for the Ti $2p_{1/2}$ is lower. The lower energy peak may be related to the strong metal- support interaction between Pt metal and TiO_2 semiconductor. This effect is associated with electron transfer from the TiO_2 support to the metal, the partly reduced Ti^{4+} at the interface between the TiO_2 and Pt metal leads to negative shift of Ti $2p_{1/2}$ peak [28, 29]. The O1s peak at a binding energy of 529.6 eV can be attributed to O^{2-} anions (lattice oxygen) in the TiO_2 in agreement with reported data [30, 31].

From Figure 8, it can be seen that, the electrochemical properties of Pt-TiO_2 films on the oxidation of CH_3OH greatly depend on the applied bias potential and the concentration of the transition metal used as dopant.

The experiment results showed that by applying a potential bias even in the presence of TiO_2 without the light (in dark), the oxidation of CH_3OH could not be initiated (the photocurrent was low), suggesting that the oxidation was photoinduced. Consequently the complete degradation of CH_3OH was caused by photocatalysis and not due to the electrochemical the oxidation. By increasing the anodic bias potential with TiO_2 under UV light, the photocurrent density increases and then reached saturation at a certain potential (about 3.5 V). Up to 3.5 V there was no increase of the photocurrent density. Then, the value of 3.5 V was selected as the best applied anodic potential bias for increasing the photocatalytic efficiency.

In the potential range of 0.5 to 5.0 V, while the undoped TiO_2 electrode exhibited lower photocurrent density, the Pt-TiO_2 electrodes exhibited noticeable photocurrent densities responses. The photocurrents of Pt-TiO_2 electrodes were much larger than that of pure TiO_2 electrode. This indicates that the photogenerated electron-hole pairs were separated more efficiently in metals-doped TiO_2 electrodes. The photocatalytic degradation of CH_3OH under UV light in aqueous solution strongly depends on the concentration of platinum metal on TiO_2. The highest photocatalytic degradation efficiency of CH_3OH was achieved with metal doping of about 1, 05 at.% concentration. The experimental results were rationalized by assuming that metal in TiO_2 lattice serves as shallow trapping sites and greatly enhancing the activity of the multi nano-porous photocatalyst. It was also observed that an increase of the concentration of transition metal in TiO_2 lead to a decrease of the photoactivity of TiO_2. The lowest photocatalytic activity was observed for the higher concentration of Pt -TiO_2 (2.23 at.%).

Figure 9 shows that the photocatalytic degradation of CH_3OH under UV light in aqueous solution strongly depends on the concentration of metal doped in TiO_2. The highest photocatalytic degradation efficiency of CH_3OH was achieved with metal doping of about 1 at.% concentration.

The experimental absorption spectra in figure 10 showed that the Pt- TiO_2 film electrodes have the ability to respond to the visible light region (537nm) while the pure TiO_2 film, which absorbs in ultraviolet region (358nm). The result clearly demonstrated that the Pt- TiO_2 thin film electrodes have a significant increase of absorbance in visible light due to platinum deposition and this is beneficial to the photocatalytic reaction of the fabricated films.

It is well known that the Schottky barrier is formed at the interface between a metal and a semiconductor. The barrier height of Pt- TiO_2 interface was estimated to be 1.65 eV from the work function of Pt (5.65 eV) and the electron affinity of TiO_2 (4.0 eV). From this calculation, it can be seen that the Schottky barrier height at Pt-TiO_2 interface is so large that there is a reduction in the mobility of electrons and holes in the conduction and valence bands respectively. The photoexcitation of electrons from the Pt metal to the conduction band of TiO_2 could take place under the irradiation of light with energy exceeding 1.65 eV in the visible absorption region [32, 33].

The platinum has an electroaffinity value of about 205.3 kJ /mol higher than titanium (7.6kJ/mol) and when TiO_2 is irradiated by UV light, the photo-produced electrons are easily transferred from TiO_2 to the Pt while the holes remain in TiO_2. This results in the charge separation of the electrons and holes from the photo-formed electron-hole pair states. Consequently, in Pt-doped TiO_2, a photoelectrochemical mechanism is predominant, in which the reduction by electrons on the metal particle and the oxidation reaction by the holes on TiO_2 occurs, respectively. The holes photoexcited in TiO_2 attach to the organics to cause a decomposition reaction. Hence the increase of the observed work function by UV irradiation can be ascribed to the trapping of the photogenerated electrons to the Pt clusters [34, 35].

A high number density of Pt nanoparticles in TiO_2 allows producing an efficient electronic state density to the energy levels, which can contribute to the photoexcitation with

lower energy than that of the band gap of anatase TiO_2, resulting in the absorption in visible light [36].

The Pt-TiO_2 thin film electrodes prepared by re-anodization method have photoresponse to visible light, which indicates a new possibility for improving TiO_2 photoresponse.

The Raman peaks in figure 11 are located around 144.4, 408.7, 511.9, and 642.1cm^{-1}, corresponding to B_{1g}, A_{1g} or B_{2g} and E_g modes of TiO_2 anatase structure [37, 38]. The peak related to rutile phase at 448,612 cm^{-1} was not observed. This result is consistent with the analysis from the XRD parttern and other analytic characterization techniques used in the present investigation, which confirm the synthesis of Pt-TiO_2 electrode. This suggests that Pt-TiO_2 electrode plays the role of accelerating the rate of methanol oxidation without itself being transformed or consumed by the reaction, acting as catalyst.

5. Conclusion

Multinanoporous thin film electrodes constituted of pure TiO_2 and the doped Pt-TiO_2 were fabricated from the titanium sheet by Re-anodization technique. They were characterized and were identified as pure TiO_2 and the doped Pt-TiO_2. The prepared Pt-TiO_2 electrodes have photoresponse to visible light, which indicates a new possibility for improving TiO_2 photoresponse.

Acknowledgements

The authors gratefully thank Dr. Xin Lihui of the National Center of Shanghai Institute of Measurement and Testing Technology for his help with SEM, TEM, FT- IR spectroscopy analysis and XRD analysis, as well as Professor Dr Shen Jianian of School of Materials Science and Engineering, Shanghai University, for his support to realize this work.

References

[1] Yan. W., Yungeng Z, Peichen L, IOP Conference Series, Earth and Environmental Science, 81 (1), (2017): 012-022.

[2] Piskalis Sahaya M K, Vinoh Kumar P, Koolath Rama K et al., J. Mater. Chem. A, 6, (2018), 23435–23444.

[3] Luis F. Arenas, Carlos Ponce de Leon, Richard P. Boardman, et al., Journal of The Electrochemical Society, 164 (2), (2017), D57-D66.

[4] Changkun Z, Hongmei Y, Yongkun L et al., Journal of Electroanalytical Chemistry 701 (2013), 14-19.

[5] Shaddad M. N., Al-Mayouf A. M., Ghanem M. A., et al., Int. J. Electrochem. Sci., 8 (2013), 2468 – 2478.

[6] Fereshteh C, Samira B, Sharifah B, et al., Sensors and Actuators B, 177 (2013), 898– 903.

[7] Agata MS, Paulina R, Kunlei W et al., Catalysts, 8 (8), (2018). 316-319.

[8] Der-Shan S, Jyh-Hwa K, Yaohsuan T et al., Nanomaterials, 6 (12), (2016), 237–239.

[9] Jadranka M, Sladana M, Nikola C et al., J. Electrochem. Soc, 165 (15), (2018), J 3253-J3258.

[10] Jinbo Z, Nan S, Faguan Z et al., RSC Advances, 7 (89), (2017), 56194-56203.

[11] Hang S. Qinrong H. Sahn Z, et al., New J. Chem 41, (2017), 7244-7252.

[12] Rettew R. E., Allam N. K., Alamgir F. M., et al., ACS Appl. Mater. Interfaces, 3, (2011), 147-149.

[13] Jinbo Z, Xuilan H, Faguan Z et al., Nanotechnology, 28 (50), (2017), 56194-56203.

[14] Košević M, Šekularac G, Živković L et al., Croat. Chem. Acta 90 (2) (2017), 251–258.

[15] Changkun Z, Hongmei Y, Yongkun et al., Journal of Electroanalytical Chemistry 701, (2013), 14–19.

[16] Shaddad M. N., Al-Mayouf A. M., Ghanem M. A., et al., Int. J. Electrochem. Sci. 8, (2013), 2468 – 2478.

[17] Susan S, Luis C Silvia, Maria E M., et al., Electrochimica Acta, 35 (6), (2017).

[18] Ekoko B. Gracien, Joseph K-K. Lobo, Omer M. Mvele et al., South African Journal of Chemistry, 66, (2013), 1-6.

[19] Ekoko B, Lobo K-K, Mvele M, et al., Pan African and South African Meeting of the International Year of Crystallography (IYCr 2014 Africa), 12-17, Octobre 2014, Bloemfontein, South Africa.

[20] Ekoko B Gracien, Jianian S, XianRong S, Dong Liu, et al, Photocatalytic activity of manganese, chromium and cobalt doped- anatase TiO_2 nanoporous electrodes produced by re-anodization method. Thin Solid Films, Vol. 515, No 13, (2007), 5287-5297.

[21] Jianian S, Moucheng L, Dong L, et al, Effects of applied bias and dopants on the photocatalytic degradation of aqueous dye solution by TiO_2/Ti electrode. Materials Science Forum, Vols. 539-543, (2007), 2240-2245.

[22] Ekoko Bakambo G., Joseph K. K. Lobo, Omer M. Mvele, et al, Effect of an external applied potential on the photocatalytic properties of manganese-doped titanium dioxide, American Journal of Physical Chemistry, 3 (4), (2014), 41-46.

[23] Toto Mabiala M, Albert Kazadi M B, Gracian Ekoko B et al, International Journal of Materials Science and Applications. 5 (5), (2016), 207-213.

[24] He Y. J., Peng J. F., Chu W et al, J. Mater. Chem. A, 2, (2014), 1721.

[25] Ismail A. A., Robben L., Bahnemann D. W, Chem Phys Chem, 12, (2011), 982.

[26] Zhang X., Zhou G, Xu J et al, Journal of Solid State Chemistry, 183 (2010), 1394–1399.

[27] Wagner, C. D. Naumkin A. V, Kraut-Vass A. et al., NIST X-ray Photoelectron Spectroscopy Database NIST Standard Reference Database 20, (2003), Version 3.5.

[28] Krstajic N. V, Vracar L. M, Radmilovic V. R, et al., Surf. Sci. 601 (2007) 1949–1966.

[29] Zhang J, Zhang M, Jin Z et al., Appl. Surf. Sci. 258 (2012) 3991–3999.

[30] Kuznetsov M. V, Ju. F. Zhuravlev, et al., J. Electron. Spectrosc. Relat. Phenom. 58 (1), (1992), 145.

[31] Mayer J. T., Diebold U, Madey T. E et al., J. Electron. Spectrosc. Relat. Phenom. 73 (1), (1995), 65.

[32] Zhao G. L, Kozuka H., Yoko T, Thin Solid Films, 277, (1996), 147-154.

[33] Li F. B., Li X. Z., Chromosphere, 48, (2002), 1103-1111.

[34] Kamat P. V, J. Phys. Chem. B, 106, (2002), 7729-7744.

[35] Kamat P. V, Pure Appl. Chem., 74, (2002), 1693-1706.

[36] Sasaki T, Koshizaki N, Yoon J. W et al., J. Photochem. Photobiol. A, 145, (2001), 11-16.

[37] Ohsaka T., Izumi F, Fujiki Y, J. Raman Spectrosc., 7, (1978), 321-324.

[38] Balachandran U, Eror N. G, J. Solid State Chem., 42, (1982), 276-282.